

ARTICLE

Corrosion testing of metals in contact with calcium chloride hexahydrate used for thermal energy storage

S. J. Ren¹  | J. Charles² | X. C. Wang² | F. X. Nie² | C. Romero² |
S. Neti² | Y. Zheng³ | S. Hoenig³ | C. Chen³ | F. Cao³ | R. Bonner³ |
H. Pearlman³

¹ Key Laboratory of Energy Thermal Conversion and Control of Ministry of Education, School of Energy and Environment, Southeast University, No. 2 Sipailou, Nanjing 210096, P. R. China

² Energy Research Center, Lehigh University, 117 ATLSS Drive, Bethlehem, Pennsylvania 18015, USA

³ Advanced Cooling Technologies, Inc., 1046 New Holland Avenue, Lancaster, Pennsylvania 17601-5688, USA

Correspondence

S. J. Ren, Key Laboratory of Energy Thermal Conversion and Control of Ministry of Education, School of Energy and Environment, Southeast University, No. 2 Sipailou, Nanjing 210096, P. R. China.

Email: rsj@seu.edu.cn

Funding information

Advanced Research Projects Agency - Energy

Thermal energy storage (TES) using a phase change material (PCM) has been proposed as a supplemental cooling system to improve the performance of power plant air-cooled condensers (ACCs). In this proposed system, frozen PCM would remove heat from plant's condensing steam during the day, which would melt the PCM. The PCM would be frozen at night as its stored heat is rejected to the cooler atmosphere. Calcium chloride hexahydrate ($\text{CaCl}_2 \cdot 6\text{H}_2\text{O}$) is an attractive material to serve as a PCM in this innovative system due to its appropriate melting temperature, low price, and relatively high latent heat of fusion. The corrosion of container materials is a major challenge in using $\text{CaCl}_2 \cdot 6\text{H}_2\text{O}$. Any material used needs to survive constant exposure to the salt for several years to ensure a long operational life for the system. In this study, the corrosion behavior of four metals in contact with $\text{CaCl}_2 \cdot 6\text{H}_2\text{O}$ was experimentally investigated. Three different temperature conditions and two pH level conditions were considered under static metal exposure conditions.

KEYWORDS

air-cooled condensers, calcium chloride hexahydrate, corrosion, phase change material, thermal energy storage

1 | INTRODUCTION

The market for air-cooled condensers (ACCs) for power generation applications has increased during the past decade due to growing water use restrictions on power plants. While ACCs are very good at reducing power plant water withdraw, this benefit is associated with a drawback caused by the steam condenser's operating temperature being dependent on the ambient air temperature.^[1] On very hot days, the condenser temperature can rise above its design condition, increasing the backpressure experienced by the low-pressure (LP) turbine

and limiting its power output. Because of this, net unit heat rate would increase, resulting in an increase in fuel consumption in order to meet demand. This problem is exasperated if the ACCs have not been adequately sized to maintain performance on the hottest days in order to reduce their size and associated capital costs.

One approach to supplement the performance of an ACC is to utilize a phase change material (PCM), which can be frozen at night and melted during the day, with the melting process removing heat from the condensate. The proposed PCM-based supplemental cooling system is presented in

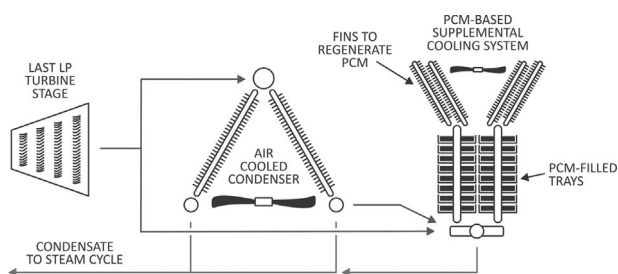


FIGURE 1 Proposed PCM-based supplemental cooling system configuration

Figure 1. This system can either be used in series with an existing ACC or be sized to entirely replace it. In this concept, heat is transferred into the PCM through a pipe connecting the PCM-filled trays. At night, this same pipe is used to transfer heat out of the PCM and into the air through fins at the top of the system.

The selection of a suitable PCM is critical to the success of the proposed enhanced ACC system, as it must meet several key criteria. First, the PCM must melt and freeze at a temperature between the nighttime temperature and the target condensate temperature. A melt/freeze temperature around 30 °C is a reasonable value, since it meets the cooling requirements for plants in regions where nighttime temperatures fall to around 20 °C. PCM cost is also critical as the expected quantity required for a full-scale system is considerable. The PCM should also have a high energy storage density, be non-hazardous and non-flammable, and maintain its performance during thousands of freezing and melting cycles. There are two major classifications of PCMs, organic PCMs, such as paraffin waxes and fatty acids; and inorganic PCMs, which are primarily hydrated salts.^[2–4] Organic PCMs offer the benefits of high energy storage capacity, little degradation after many operating cycles and minimal corrosiveness. Inorganic PCMs are typically an order of magnitude less expensive than organics, offer high energy storage capacities, and are non-flammable.^[5] Some known issues with inorganic PCMs are that they can degrade over time, they tend to be highly corrosive, and they typically require additives to prevent supercooling. However, since PCM cost is a first consideration for this proposed system, inorganic PCMs are considered to be the first choice.

$\text{CaCl}_2 \cdot 6\text{H}_2\text{O}$ was selected for the study reported in this paper as a prime PCM candidate due to its melting temperature between 27.5 and 30.2 °C,^[6] with a relatively high latent heat of melting/freezing of approximately 175 J/g.^[7] Cost is also known to be very low for this PCM.^[8,9] In addition, Tyagi and Buddhi^[10] have reported that $\text{CaCl}_2 \cdot 6\text{H}_2\text{O}$ has shown considerable stability in both its heat of fusion and melt temperature throughout the duration of 1000 thermal cycles. Although, $\text{CaCl}_2 \cdot 6\text{H}_2\text{O}$ is a suitable PCM from a thermal, cost, and safety standpoint, because it is

a chloride-based salt, it is known to be highly corrosive. In the concept system presented in Figure 1, commercial PCM-based supplemental cooling system will need to contain the PCM in low-cost, easy to manufacture trays; having a low thermal resistance, in order to efficiently transfer heat between the condensate pipe and the metal PCM trays. This means that the corrosion of any proposed metal in close contact with $\text{CaCl}_2 \cdot 6\text{H}_2\text{O}$, is of critical importance in ensuring long-term, reliable operation of the system.

This paper reports results of an investigation into the corrosion behavior of different metals, under static exposure to $\text{CaCl}_2 \cdot 6\text{H}_2\text{O}$. Four metals (copper, 1018 (A36) carbon steel, aluminum (Al 6061, and Al 5086)) were selected and their corrosion rates were evaluated through experiments, with a duration of up to 16 weeks. Three different test temperatures (30, 50, and 80 °C) and two different pH levels (3.5 and 5.5) were considered to estimate the corrosion performance of the four metals exposed to $\text{CaCl}_2 \cdot 6\text{H}_2\text{O}$.

2 | MATERIALS AND METHODS

2.1 | Phase change material

Before being investigated for its corrosion potential, $\text{CaCl}_2 \cdot 6\text{H}_2\text{O}$ was tested by differential scanning calorimetry (DSC) to determine its thermal performance during melting and freezing. Samples of $\text{CaCl}_2 \cdot 6\text{H}_2\text{O}$ of between 15 and 25 mg were slowly heated from –30 to 50 °C in a DSC using a 7 °C/min heating rate. The DSC is able to record the heat flow into and out of the sample during this heating process. Figure 2 presents a typical DSC melting curve generated for $\text{CaCl}_2 \cdot 6\text{H}_2\text{O}$. It can be seen that as the temperature rises above 20 °C, a dramatic increase in the heat flow out of the sample indicates that the PCM is melting. The point where maximum heat flow occurs is defined as the peak melting temperature, which is ~33.69 °C for the case shown. It is thought that this peak temperature does not correspond to the melting temperature

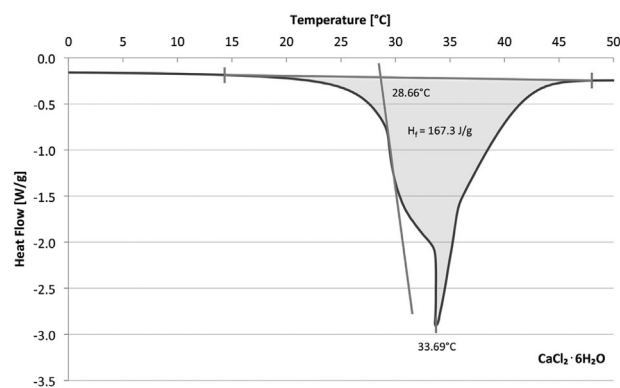


FIGURE 2 DSC melting test of $\text{CaCl}_2 \cdot 6\text{H}_2\text{O}$

TABLE 1 $\text{CaCl}_2 \cdot 6\text{H}_2\text{O}$ thermal properties as determined from three DSC tests

PCM	Manufacturer	Purity	Peak temp. [°C]	Melting temp. [°C]	Heat of fusion of melting [kJ/kg]
$\text{CaCl}_2 \cdot 6\text{H}_2\text{O}$	Acros Organics	99% +	33.0	27.5–30.2 ^[6]	170.5 ± 10.7

of the PCM, but rather the onset temperature (28.66 °C in Figure 2) is more representative of the average melt temperature. The onset temperature is calculated by drawing a line tangent to the heat flow curve at the point with the steepest slope. The intersection point between this line and a straight line connecting the pre-melt and post-melt heat flow curves is defined as the onset temperature (see Figure 2). The area contained within the heat flow curve and this straight line is equivalent to the total heat released during the melting process (latent heat of melting of the PCM). Thermal results from three DSC tests of $\text{CaCl}_2 \cdot 6\text{H}_2\text{O}$ were averaged and are presented in Table 1.

2.2 | Metals

Four metals were selected as potential PCM tray materials: copper, Al 6061, Al 5086, and 1018 (A36) carbon steel. The appearance of these metals prior to corrosion is presented in Figure 3. The chemical compositions of the metals are summarized in Table 2. All of the metals were cut into coupons measuring 50.8 mm in length by 12.7 mm wide and 1.6 mm thick.

2.3 | Mass loss corrosion rate measurement methodology

The corrosion experiments were conducted according to the ASTM G1-03 guideline.^[11] The following steps were adopted based on this method and were found to provide reproducible corrosion results:

2.3.1 | Step 1: Sample preparation

Test coupons were cut from 1.6 mm thick metal sheets to a desired width of 12.7 mm and length of 50.8 mm. After each coupon was uniquely labeled, they were polished with a wire

wheel to both clean the surface and remove any rough edges. Next, acetone and hot air were used to degrease and dry the specimens, respectively. Each cleaned and dried coupon was then weighed to a precision of 0.1 mg before immersion into glass bottles filled with liquid $\text{CaCl}_2 \cdot 6\text{H}_2\text{O}$. The glass bottles were capped to prevent exposure of the PCM to the environment. Sealing of the PCM is critical as hydrated salts are known to either absorb water from or release water into air, depending on the air's humidity and the composition of the salt.

2.3.2 | Step 2: Corrosion characterization tests

The coupons immersed in $\text{CaCl}_2 \cdot 6\text{H}_2\text{O}$ were selectively placed into three heating chambers at different operating temperatures, 30, 50, and 80 °C. The 30 °C condition was selected as it corresponds to the melting temperature of the PCM. The higher temperature conditions were selected to determine the impact of temperature on accelerating the corrosion rate. By knowing the effect of temperature on the corrosion rate, future corrosion tests could be conducted over a reduced timeframe, with the results from these accelerated tests referred back into real-time results. Twenty-four coupons were prepared for each metal, which allowed for two coupons (to compare with one another to ensure reproducible results) to be removed at each of four test durations (2, 4, 8, and 16 weeks) for all three temperatures.

2.3.3 | Step 3: Sample cleaning and weighing

After the coupons were removed from the $\text{CaCl}_2 \cdot 6\text{H}_2\text{O}$ containers at 2, 4, 8, and 16 weeks, they were chemically cleaned following the ASTM G1-03 method. Table 3 presents the chemicals and their composition for coupon cleaning. After cleaning the coupons, they were placed in reagent water and lightly brushed to remove any

**FIGURE 3** Photographs of four metals prior to corrosion testing

TABLE 2 Composition of selected metals

Element/metal	Copper	A36 carbon steel	Aluminum 5086	Aluminum 6061
% Al	–	–	Bal.	Bal.
% C	–	Max 0.26	–	–
% Cr	–	–	0.05–0.25	0.04–0.35
% Cu	99.9	–	Max 0.1	0.15–0.40
% Fe	–	Bal.	Max 0.5	Max 0.7
% Mg	–	–	3.5–4.5	0.8–1.2
% Mn	–	Max 0.75	0.2–0.7	Max 0.15
% Ni	–	–	–	–
% P	–	Max 0.04	–	–
% S	–	Max 0.05	–	–
% Si	–	–	Max 0.4	0.4–0.8
% Ti	–	–	Max 0.15	Max 0.15
% Zn	–	–	Max 0.25	Max 0.25
Density (g/cm ³)	8.96	7.85	2.7	2.7

remaining loose corrosion particles. Finally, the coupons were dried with hot air and weighed to determine their mass loss during the corrosion test period.

2.3.4 | Step 4: Data collection and analysis

The measured mass loss of the coupons due to corrosion was used to calculate the metal's corrosion rate according to Eq. (1).^[11]

$$\text{Corrosion Rate} = k \frac{\Delta m}{\rho S t} \quad (1)$$

where Δm is the change in mass of the coupon due to corrosion, ρ is the density of the metal coupon, S is the surface area of the coupon, t is the corrosion test duration, and k is a conversion factor to convert the corrosion rate into the desired units. The corrosion rate can be used as an indicator of the long-term stability of the metal in the presence of $\text{CaCl}_2 \cdot 6\text{H}_2\text{O}$. Table 4 presents an industrial guide for corrosion rate and how it correlates to metal durability.^[12]

2.4 | Method for evaluation of pitting corrosion

Pitting is a form of localized corrosion that produces defects (pits) of considerable depth in small areas. If these pits become sufficiently deep, the metal may be breached without there being significant corrosion across the majority of the surface. Because of this, the metal mass loss cannot accurately determine the degree of pitting damage unless general corrosion is negligible and pitting is severe. Therefore, in order to note the degree of coupon corrosion due to pitting, the corroded coupons, after being chemically cleaned, were manually examined under a magnifying glass. This analysis was conducted according to the ASTM G 46-94 method.^[13]

2.5 | Modification of PCM pH to note effect on corrosion rate

In order to investigate the effect of pH on corrosion behavior, calcium hydroxide (CaOH) powder was used to modify the pH level of $\text{CaCl}_2 \cdot 6\text{H}_2\text{O}$ from 3.5 to 5.5. Three metals (A36 carbon steel, Al 5086, and Al 6061) were selected to be tested at a pH = 5.5 for the modified $\text{CaCl}_2 \cdot 6\text{H}_2\text{O}$ salt, at 50 °C for 2 and 4 weeks.

TABLE 3 Chemicals used to clean metals after corrosion testing – according to ASTM G1-03 method

Metal	Solution	Immersion time	Immersion temp.
Carbon steel	(1) 500 ml hydrochloric acid (HCl, sp. gr. 1.19)	10 min	20–25 °C
	(2) 3.5 g hexamethylene tetramine		
	(3) Reagent water to make 1000 ml		
Copper	(1) 500 ml hydrochloric acid (HCl, sp. gr. 1.19)	1–3 min	20–25 °C
	(2) Reagent water to make 1000 ml		
Al 6061/5086	(1) Nitric acid (HNO ₃ , sp. gr. 1.42)	1–5 min	20–25 °C

TABLE 4 Industry guide for corrosion rate based on mass loss measurements^[12]

mg/cm ² yr	mm/yr	mills/yr	Recommendation
>1000	2	78.7	Completely destroyed within days
100–999	0.2–1.99	7.9–78.6	Not recommended for service greater than a month
50–99	0.1–0.19	3.9–7.8	Not recommended for service greater than a year
10–49	0.02–0.09	0.8–3.8	Caution recommended, based on the specific application
0.3–9.9	–	–	Recommended for long-term service
<0.2	–	–	Recommended for long-term service; no corrosion, other than as a result of surface cleaning, was evident

3 | RESULTS AND DISCUSSION

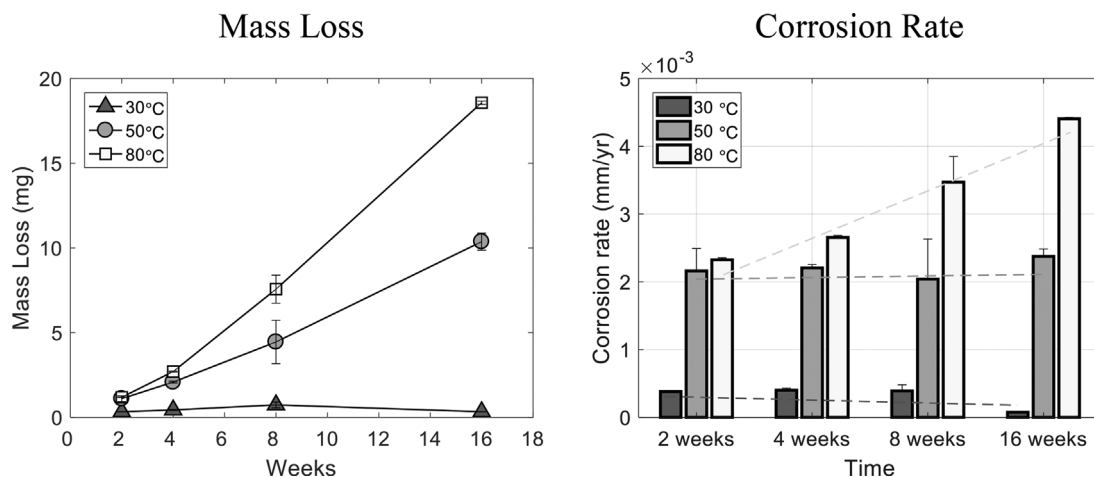
3.1 | Mass-loss and pitting results for PCM-metal pairs

Figure 4 presents both mass loss and corrosion rate test results for copper immersed in liquid $\text{CaCl}_2 \cdot 6\text{H}_2\text{O}$ at the three test temperatures. These results show that the corrosion rate of copper is highly dependent on temperature. Copper test results at 30 °C show a very low mass loss and corrosion rate for all test times. The slight decrease in mass loss at 16 weeks is thought to be due to the fact that the measured mass losses were close to the measurement uncertainty of the balance. The experiments at 50 °C show a nearly linear increase in mass loss with time, resulting in little change in the corrosion rate with increasing time. However, for the 80 °C samples, the corrosion rate increased significantly with time. These results also show that both mass loss and corrosion rate consistently increase with increasing temperature. This phenomenon was also visually observed in the sample bottles. Figure 5 shows the copper coupons immersed in $\text{CaCl}_2 \cdot 6\text{H}_2\text{O}$ after 16 weeks. It can be seen, that at 30 °C, the PCM was observed to be entirely clear. At 50 °C, a slight blue tint is observed due to corrosion products in the PCM. At 80 °C, the corrosion products have formed a vivid blue layer on the top of the

PCM. No pitting corrosion was observed on the copper coupons for all three temperature conditions.

Corrosion test results for A36 carbon steel immersed in $\text{CaCl}_2 \cdot 6\text{H}_2\text{O}$ are presented in Figure 6. Although the mass loss of carbon steel is seen to increase with time, the corrosion rate decreases with time during the 16-week test period. It is thought that the formation of an oxide layer on the surface of the steel acts as a protective layer over the steel, slowing the corrosion progress as time progresses under exposure to the chlorine salt. During these tests, the color of the PCM solution gradually changed from transparent to pale yellow under all three temperatures, and some dark precipitate was observed in the 50 and 80 °C solutions after 16 weeks (Figure 7). There was no evidence of pitting corrosion on any of the A36 carbon steel coupons.

Figure 8 shows that the mass loss of the Al 5086 samples increases with time, while the corrosion rate decreases with time for all three temperatures. This is not surprising as aluminum is known to form a protective oxide layer that is particularly effective at preventing further corrosion. As with the other metals, the higher temperatures correspond to larger mass loss and higher corrosion rates at all immersion periods. Moreover, significant changes in the solutions were observed. Soon after the beginning of the corrosion tests, many small air

**FIGURE 4** Mass loss (left) and corrosion rate (right) of copper in $\text{CaCl}_2 \cdot 6\text{H}_2\text{O}$ at 30, 50, and 80 °C

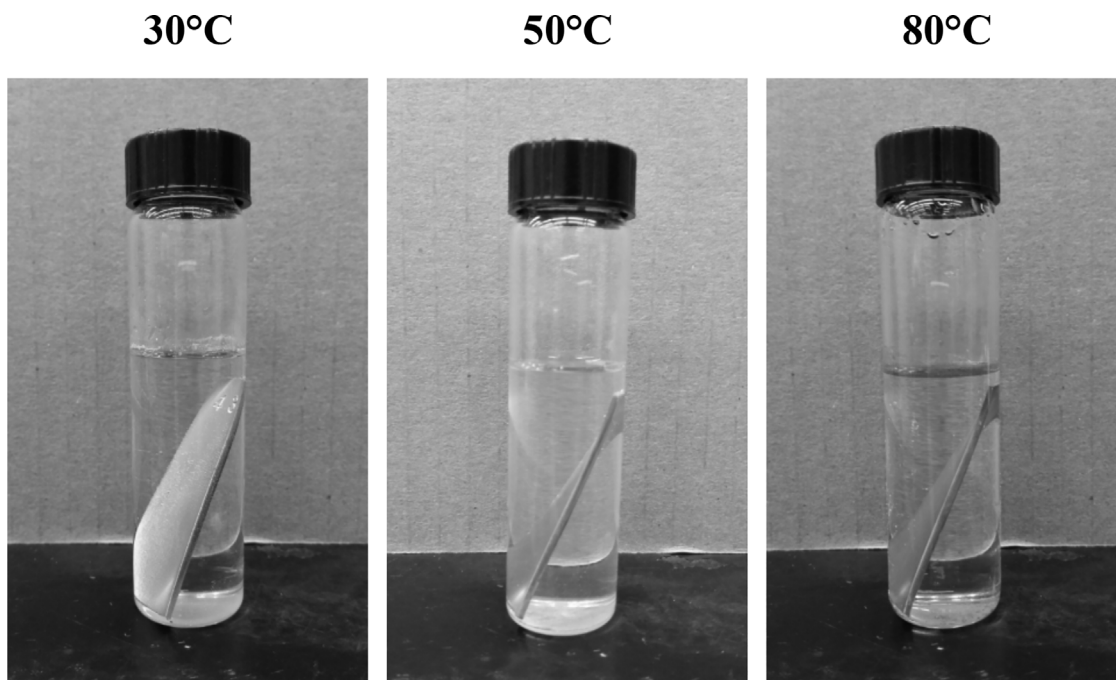


FIGURE 5 Copper coupons in test bottles after 16 weeks

bubbles were observed to be uniformly distributed across the coupons' surfaces. As time progressed, some white emulsion began to appear on the surface, while the number of air bubbles decreased. After 16 weeks, the surfaces of all of the Al 5086 coupons were entirely covered with a white emulsion, and very few bubbles were observed, as seen in Figure 9. Finally, no evidence of pitting was observed on the Al 5086 coupons tested at 30 °C for 16 weeks (Figure 10). However, minimal pits were observed on the coupons immersed in both the 50 and 80 °C PCM. Both the number and size of pits were seen to increase with increased time at the test temperature.

Al 6061 is also known to form a protective oxide layer. This is evident in the measured decrease in corrosion with increasing test duration (Figure 11). As expected, greater mass loss and an increased corrosion rate were observed as the temperature was increased. Figure 12 clearly shows that air bubbles were observed on the coupon surfaces in the solution for all three temperatures. Additionally, Al 6061 suffered from significant pitting corrosion under all three temperature conditions. When the temperature was 30 or 50 °C, a few small pits were observed on the Al 6061 specimens after 16 weeks of corrosion testing (Figure 13). When the temperature was increased to 80 °C, pits started to appear

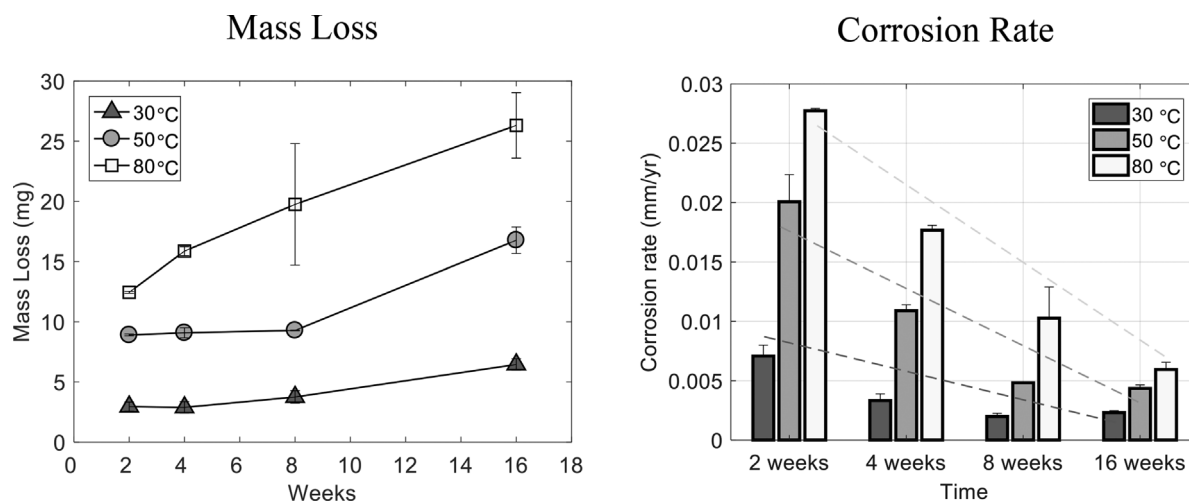


FIGURE 6 Mass loss (left) and corrosion rate (right) of carbon steel in $\text{CaCl}_2 \cdot 6\text{H}_2\text{O}$ at 30, 50, and 80 °C

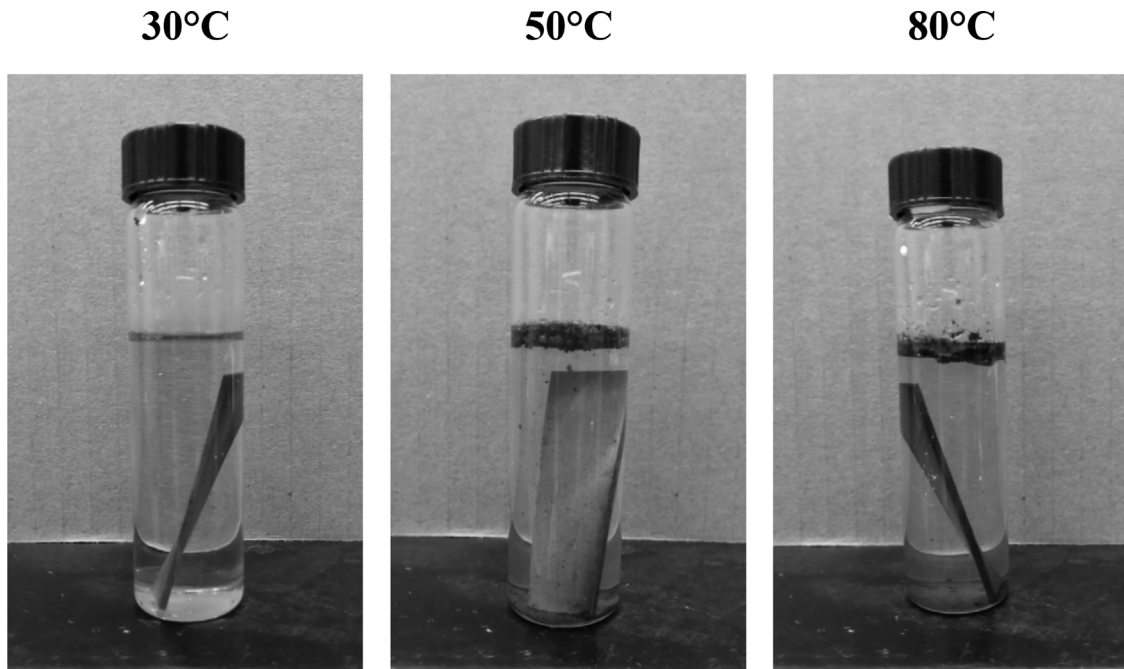


FIGURE 7 Carbon steel coupons in test bottles after 16 weeks

after 4 weeks, and the size of pits increased with increasing time.

3.2 | Temperature dependence of corrosion rate

A pseudo Arrhenius equation was used to correlate the temperature dependence of the corrosion rate after 16 weeks of testing in $\text{CaCl}_2 \cdot 6\text{H}_2\text{O}$ for four different metals:

$$\ln K = \frac{-E_a}{RT} + \ln A \quad (2)$$

where, K is the corrosion rate, E_a is an apparent activation energy, A is the Arrhenius constant, R is the gas constant, and T is the absolute temperature.

By plotting $\ln K$ versus $1/T$, linear curve fits of the data can be obtained to find E_a . Figure 14 presents $\ln K$ versus $1/T$ curves for all four metals. Calculated E_a values are presented in Table 5 along with the linear regression coefficients for the curve fits shown in Figure 14. Since all of the regression coefficients are very close to 1, it can be said that these corrosion tests follow a given Arrhenius relationship.

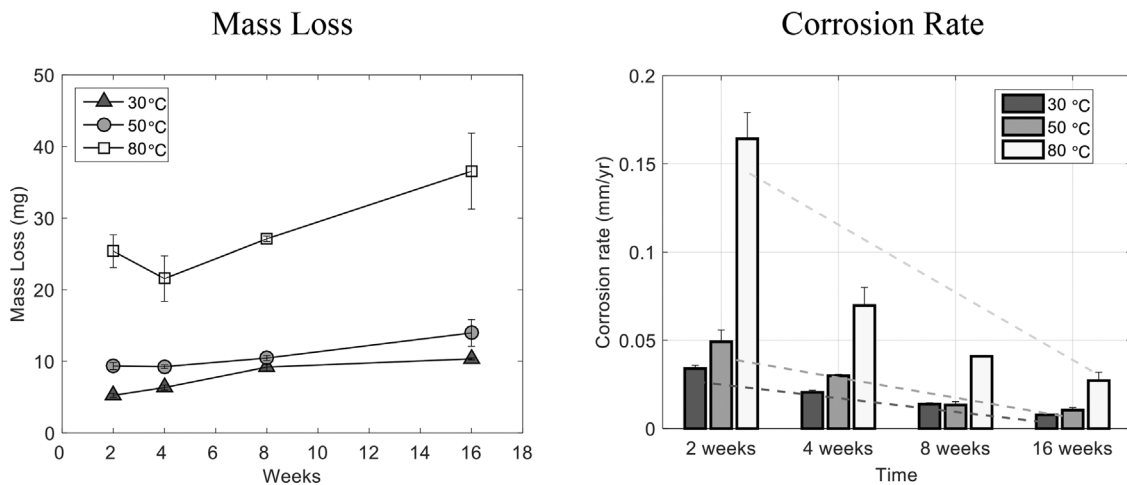


FIGURE 8 Mass loss (left) and corrosion rate (right) of Al 5086 in $\text{CaCl}_2 \cdot 6\text{H}_2\text{O}$ at 30, 50, and 80 °C

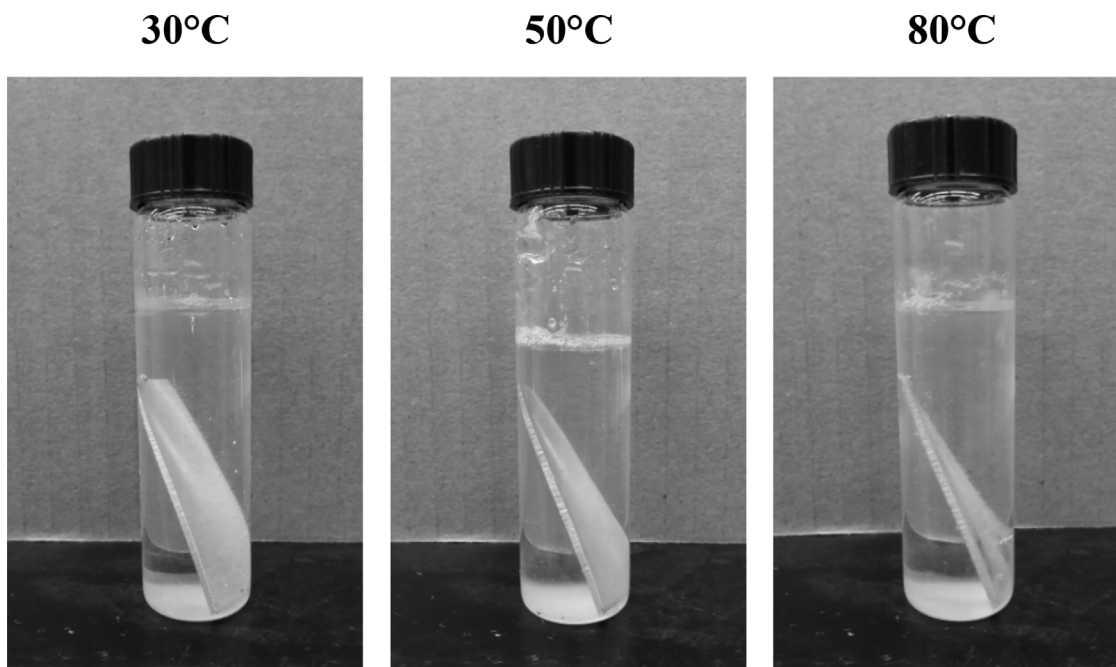


FIGURE 9 Al 5086 coupons in test bottles after 16 weeks in $\text{CaCl}_2 \cdot 6\text{H}_2\text{O}$

3.3 | Effect of PCM pH on corrosion rate

The pH of $\text{CaCl}_2 \cdot 6\text{H}_2\text{O}$ was increased from around 3.5 to 5.5 through the addition of CaOH . Corrosion testing of A36 carbon steel, Al 6061, and Al 5086 was conducted in this high pH PCM for test durations of 2 and 4 weeks. Figures 15 through 17 present corrosion rate results for these three metals in $\text{CaCl}_2 \cdot 6\text{H}_2\text{O}$ at the two pH levels. All samples were tested at 50 °C for 2 and 4 weeks. Figure 15 shows that the corrosion

rate of carbon steel appears to be lower at a pH of 5.5 after 4 weeks of testing. However, it should be cautioned that the corrosion rates of carbon steel in $\text{CaCl}_2 \cdot 6\text{H}_2\text{O}$ at 50 °C are very low and these results may not apply if the corrosion rate were higher or the timescale much longer.

For Al 5086 and Al 6061, Figures 16 and 17 show that increasing the pH increased the corrosion rate for all test durations. This was contrary to what was expected, but it is important as it clearly illustrates that there is little motivation

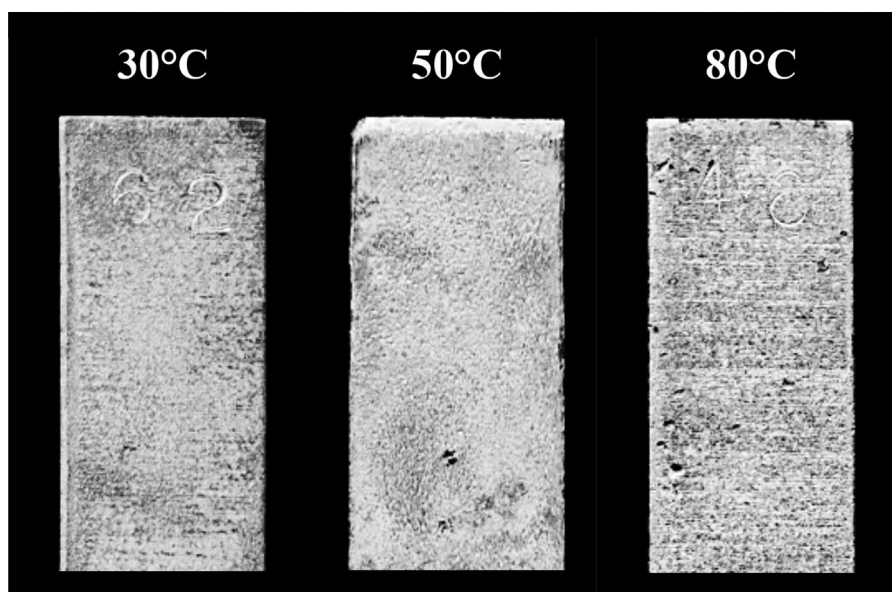


FIGURE 10 Pitting of Al 5086 coupons after 16 weeks in $\text{CaCl}_2 \cdot 6\text{H}_2\text{O}$

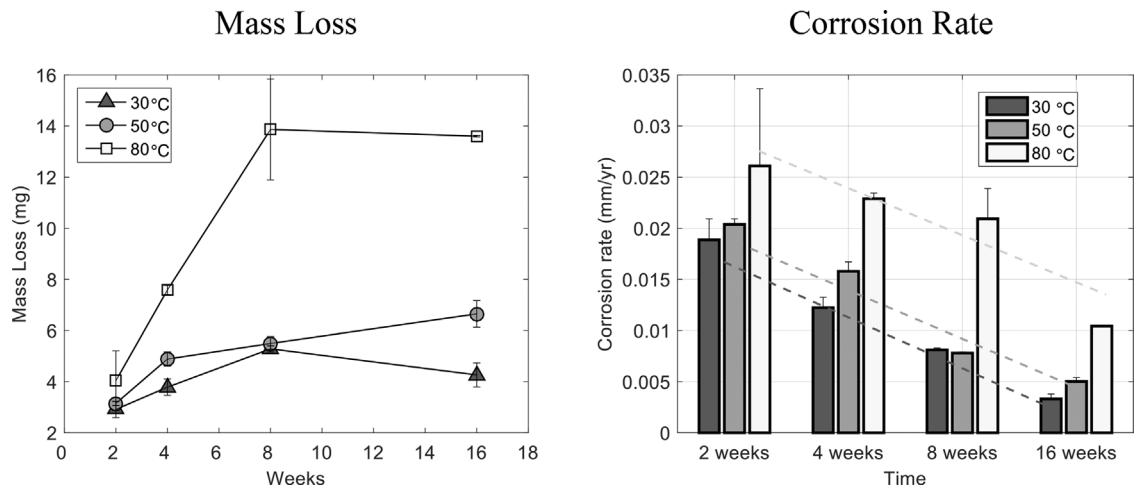


FIGURE 11 Mass loss (left) and corrosion rate (right) of Al 6061 in $\text{CaCl}_2 \cdot 6\text{H}_2\text{O}$ at 30, 50, and 80 °C

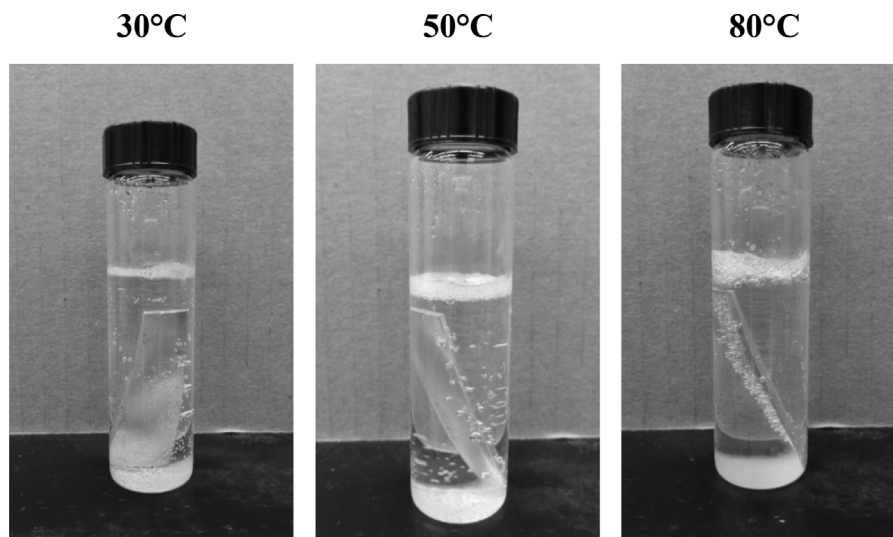


FIGURE 12 Al 6061 coupons in test bottles after 16 weeks in $\text{CaCl}_2 \cdot 6\text{H}_2\text{O}$

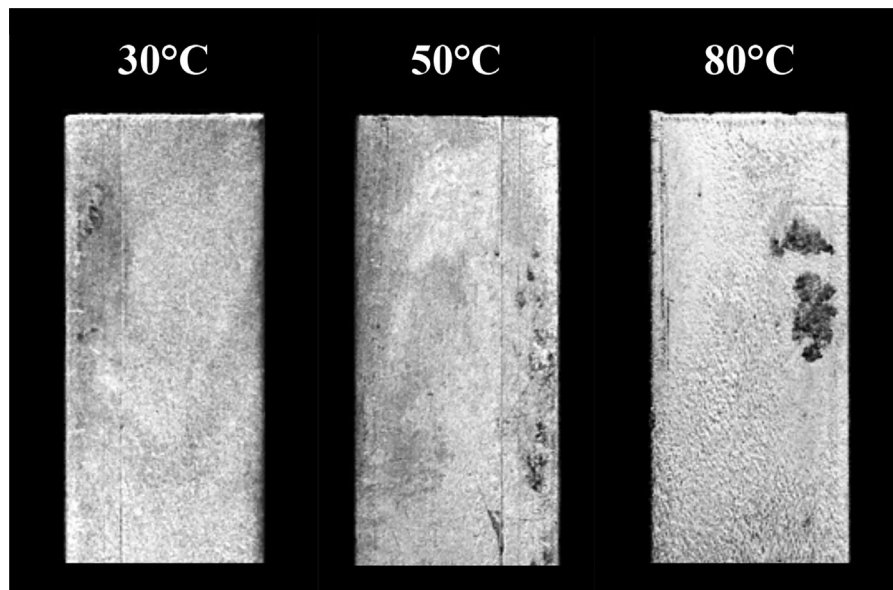


FIGURE 13 Pitting of Al 6061 coupons after 16 weeks in $\text{CaCl}_2 \cdot 6\text{H}_2\text{O}$

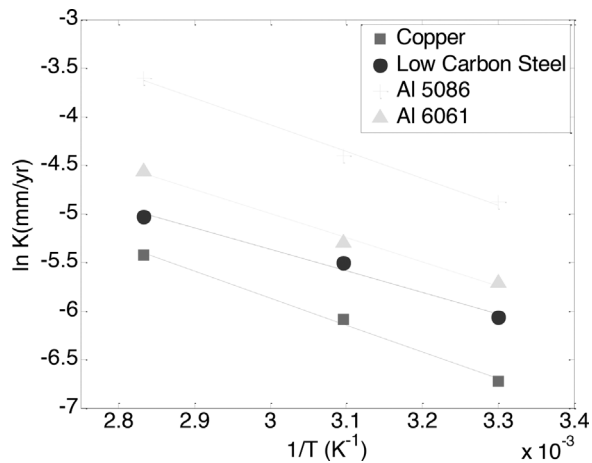


FIGURE 14 Arrhenius curves for four metals in $\text{CaCl}_2 \cdot 6\text{H}_2\text{O}$

for tuning the pH of $\text{CaCl}_2 \cdot 6\text{H}_2\text{O}$ to reduce the corrosion rate of any aluminum it comes in contact with.

4 | CONCLUSIONS

$\text{CaCl}_2 \cdot 6\text{H}_2\text{O}$ is a promising PCM for low temperature heat storage, which can be utilized in improving the efficiency of air-cooled power plants. For this hydrated salt to be used, any container (encapsulation material) used to contain it must resist corrosion by the salt throughout the system's life. Long-term corrosion tests of $\text{CaCl}_2 \cdot 6\text{H}_2\text{O}$ in contact with four common metals (copper, low carbon steel, Al 5086, and Al 6061) were performed. The corrosion tests were carried out for four test periods (2, 4, 8, and 16 weeks), and three temperature conditions (30, 50, and 80 °C). The important findings of these tests are as follows:

(1) *Effect of time on corrosion rate.* For all temperature conditions, the corrosion rates of carbon steel, Al 5086, and Al 6061, were found to decrease as test time increased. This was expected as it is well known that corrosion rates begin to slow down as a protective oxide layer forms on the surface of the metal. Interestingly, copper did not follow this trend, with the corrosion rate of copper increasing with time for the 80 °C temperature condition.

TABLE 5 Activation energy for four metals in contact with $\text{CaCl}_2 \cdot 6\text{H}_2\text{O}$

Metal	E_a [kJ/mol]	Linear regression coefficient
Copper	23.01	0.9959
A36 carbon steel	18.35	0.9859
Al5086	20.54	0.9949
Al6061	22.79	0.9927

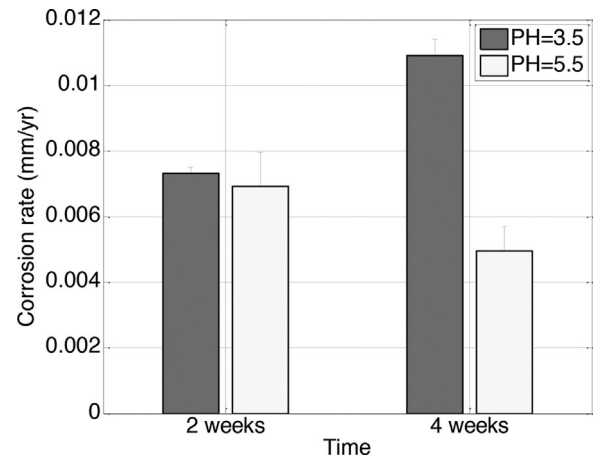


FIGURE 15 Effect of pH on A36 carbon steel corrosion rate

- (2) *Effect of temperature on corrosion rate.* While temperature is known to accelerate corrosion in many situations, its impact on the corrosion rate of metals immersed in $\text{CaCl}_2 \cdot 6\text{H}_2\text{O}$ has not been reported in the literature. Testing of the four metals at 30, 50, and 80 °C confirmed the hypothesis that an increase in temperature results in an increase in the corrosion rate for each of the metals. Plotting the natural log of the corrosion rate versus $1/T$, these test results were shown to follow an Arrhenius relationship, with apparent activation energies for the corrosion reactions being found.
- (3) *Pitting corrosion.* While the ASTM G1-03 corrosion method has been often used to quantify the corrosion rate of metals in the presence of hydrated salt PCMs, this method cannot quantitatively measure pitting corrosion of the sample. Visual observation of the samples showed no pitting of the copper and carbon steel samples under all three temperature conditions. Al 5086 suffered serious

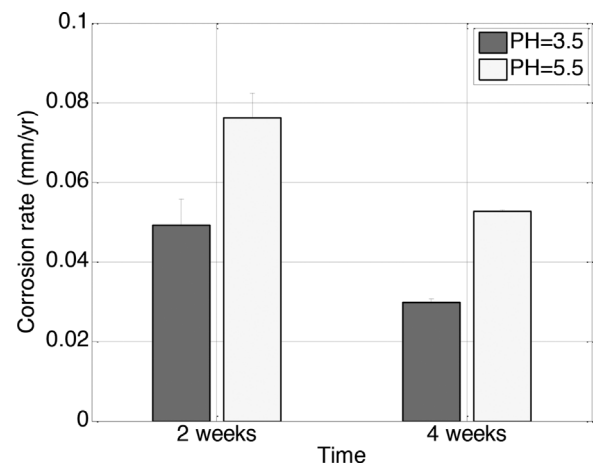


FIGURE 16 Effect of pH on Al 5086 corrosion rate

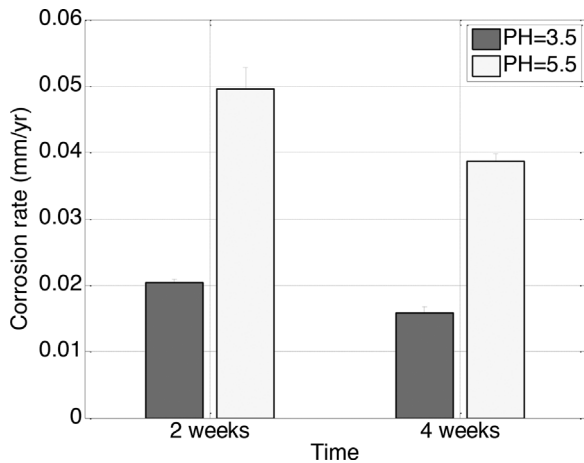


FIGURE 17 Effect of pH on Al 6061 corrosion rate

pitting corrosion only at 80 °C, while pitting of the Al 6061 samples was observed at all three temperatures. Pitting size and depth was found to be directly proportional to temperature.

- (4) *Effect of pH on corrosion rate.* It was hypothesized that the pH of the PCM should have an impact on the corrosion rate. With the effect of pH on the corrosion rate of metals in the presence of $\text{CaCl}_2 \cdot 6\text{H}_2\text{O}$ being unknown, tests were conducted where the baseline pH of $\text{CaCl}_2 \cdot 6\text{H}_2\text{O}$ (~3.5) was increased to around 5.5 through the addition of CaOH. Corrosion tests of A36 carbon steel, Al 5086, and Al 6061 at this elevated pH showed that each metal responds differently to the increase in pH. For the aluminum samples, increasing PCM pH from 3.5 to 5.5 increases the corrosion rate by around 100%. For carbon steel, the increase in pH resulted in around a 50% reduction in the corrosion rate at a test duration of 4 weeks.
- (5) *Recommendations.* A36 carbon steel has been found to have a very low corrosion rate in the presence of liquid $\text{CaCl}_2 \cdot 6\text{H}_2\text{O}$ (<0.0025 mm/yr) for a test duration of 16 weeks at a temperature equal to the target PCM melting temperature (~30–32 °C). Copper performs even better (< 2×10^{-5} mm/yr at 30 °C and 16 weeks), but its high cost (\$/kg) most likely precludes its use in this application. Aluminum 5086 has a higher corrosion rate of <0.02 mm/yr at 30 °C and 16 weeks, but it may still prove to be an acceptable material option as long as the maximum PCM temperature does not exceed 50 °C. Al 6061 is not recommended due to the observation of

pitting corrosion at all test temperatures. For aluminum, a lower pH (~3.5) has been found to result in a lower corrosion rate, while a higher pH (up to 5.5) has been found to lower the corrosion rate of A36 carbon steel.

ACKNOWLEDGMENT

Financial support for this research was provided by the Energy Department's Advanced Research Projects Agency-Energy (ARPA-E), and is gratefully acknowledged.

REFERENCES

- [1] J. G. Bustamante, A. S. Rattner, S. Garimella, *Appl. Therm. Eng.* **2016**, *105*, 362.
- [2] W. Zhao, D. M. France, W. Yu, T. Kim, D. Singh, *Renew. Energy*. **2014**, *69*, 134.
- [3] G. Li, Y. Hwang, R. Radermacher, *Int. J. Refrig.* **2012**, *35*, 2053.
- [4] A. Gil, M. Medrano, I. Martorell, A. Lazaro, P. Dolado, B. Zalba, L. F. Cabeza, *Renew. Sustain. Energy Rev.* **2010**, *14*, 31.
- [5] A. Sharma, V. V. Tyagi, C. R. Chen, D. Buddhi, *Renew. Sustain. Energy Rev.* **2009**, *13*, 318.
- [6] S. M. Hasnain, *Energ. Convers. Manage.* **1998**, *39*, 1127.
- [7] K. Kaygusuz, *Energy Sources* **1999**, *21*, 745.
- [8] H. Fellchenfeld, S. Sarig, *Ind. Eng. Chem. Prod. Res. Dev.* **1985**, *24*, 130.
- [9] B. Carlsson, *Sol. Energy*. **2009**, *83*, 485.
- [10] V. V. Tyagi, D. Buddhi, *Sol. Energy Mater. Sol. Cells* **2008**, *92*, 891.
- [11] *ASTM International G 1-03*, **2003**, Standard Practice for Preparing, Cleaning, and Evaluation Corrosion Test Specimens.
- [12] L. F. Cabeza, G. Svensson, S. Hiebler, H. Mehling, *Appl. Therm. Eng.* **2003**, *23*, 1697.
- [13] *ASTM International G 46-94*, **2005**, Standard Guide for Examination and Evaluation of Pitting Corrosion.

How to cite this article: Ren SJ, Charles J, Wang XC, et al. Corrosion testing of metals in contact with calcium chloride hexahydrate used for thermal energy storage. *Materials and Corrosion*. 2017;1–11. <https://doi.org/10.1002/maco.201709432>